https://doi.org/10.31436/iiumej.v27i3.4503

CFD Analysis of the Effect of a Ball Throttle on the Hydraulic Drive Stability

GULSARA ANNAKULOVA, SARVAR SAIDOV*, BEKZOD ASTANOV

Department of Mechanics of Fluids, Gas and Drive Systems, Institute of Mechanics and Seismic Stability of Structures named after M.T. Urazbaev, Uzbekistan Academy of Sciences, Tashkent, Uzbekistan

**Corresponding author: sarvarsaid1987@gmail.com*

(Received: 4 June 2026; Accepted: 13 August 2026; Published online: 11 September 2026)

ABSTRACT: This paper investigates the impact of a ball throttle on the stability of a vehicle's hydraulic drive system. To do so, a simulation model of the hydraulic system was developed in MATLAB/Simulink, and a 3D computational fluid dynamics (CFD) analysis of the working fluid flow was conducted in SolidWorks Flow Simulation. Additionally, experimental studies were performed on a KI-4815M hydraulic test bench, utilizing SS302 pressure sensors and an Arduino-based data acquisition system. The findings indicate that implementing a ball throttle helps reduce pressure fluctuations and dynamic loads within the hydraulic system. The differences between the CFD results, Simulink simulations, and experimental data do not exceed 5,67% at a load of 700 N. These results confirm the effectiveness of the proposed method for enhancing the stability of hydraulic drives.

ABSTRAK: Kajian ini menyelidiki kesan pendikit bola terhadap kestabilan sistem pemacu hidraulik kenderaan. Bagi mencapai tujuan ini, satu model simulasi sistem hidraulik telah dibangun menggunakan MATLAB/Simulink, manakala analisis dinamik bendalir pengiraan (CFD) 3D bagi aliran bendalir kerja telah dilakukan mengguna pakai simulator SolidWorks Flow. Selain itu, kajian eksperimen telah dilaksanakan pada bangku ujian hidraulik KI-4815M dengan penderia tekanan SS302 serta sistem pemerolehan data berasaskan Arduino. Dapatan kajian menunjukkan bahawa pelaksanaan pendikit bola membantu mengurangkan turun naik tekanan dan beban dinamik dalam sistem hidraulik. Perbezaan antara keputusan CFD, simulasi Simulink, dan data eksperimen tidak melebihi 5.67% pada beban 700 N. Dapatan ini mengesahkan keberkesanan kaedah yang dicadangkan dalam meningkatkan kestabilan pemacu hidraulik.

KEYWORDS: *hydraulic systems, ball throttle, flow control, CFD (computational fluid dynamics), CAD (computer-aided design).*

1. INTRODUCTION

A machine-controlled hydraulic drive is a volumetric hydraulic drive in which a variable-speed pump or variable-speed hydraulic motor regulates the output link motion parameters. In a drive-motor-controlled hydraulic drive, the drive motor's speed controls the output link motion parameters. Furthermore, a throttle-controlled hydraulic drive operates with output link motion parameters governed by a regulating hydraulic device. A machine-throttle-controlled hydraulic drive combines these two approaches, controlling the output link motion parameters using both a regulating hydraulic device and a volumetric hydraulic machine [1].

Determining pressure drops and resistance losses is essential for ensuring the stability and robustness of hydraulic drives. In hydraulic systems, pressure fluctuations or flow irregularities can cause actuator instability, reduce hydraulic cylinder positioning accuracy, and shorten the service life of pumps and valves.

Classic analytical methods for calculating hydraulic drives do not always account for the complex effects of turbulence, swirl, and throttle geometry, which directly affect the system's stability and stable operation. Computational fluid dynamics (CFD) methods are currently widely used to analyze the internal flow structure, pressure distribution, and hydrodynamic forces in hydraulic valves. In recent years, CFD modeling has become a key tool for improving the reliability and efficiency of servo valves and control valves by more accurately describing complex transient processes. It enables numerical calculation of velocity and pressure drop (ΔP) in complex flows, and prediction of pulsation and swirl zones that can cause instability in hydraulic drives [2-4].

Hydraulic systems in vehicles – pumps, hydraulic motors, hydraulic cylinders, valves, and associated lines – must meet requirements for high efficiency, reliability, and cost-effectiveness. CFD can analyze pressure losses, cavitation, and processes dependent on external conditions. For example, CFD can more accurately calculate flow forces around a moving valve spool [5]. One advantage of CFD is virtual prototyping, which can significantly reduce the time and cost of physical testing (e.g., of a pump or cylinder) [6].

In [7], the internal leakage processes in the main cascade of a servo valve were investigated using 2D CFD modeling. The study found that leakage occurs predominantly through the gap and increases nonlinearly with increasing pressure drop. In [8], a three-dimensional unsteady CFD analysis of the hydrodynamic forces acting on the spool of a control valve was carried out. It was shown that 3D modeling allows more accurate consideration of flow asymmetry and dynamic oscillations than the 2D case. In [9], approaches to reducing hydrodynamic forces on the spool through geometric optimization of the flow path were proposed, improving valve-operation stability. In [10], the authors analyzed flow-pressure characteristics and showed the influence of geometry and flow regimes on valve-operation stability. In [11], a dynamic model of a direct-drive rotary servo valve was developed, confirming its high response speed and control accuracy. A study in [12] analyzed relief-valve stability and showed that hydrodynamic vibrations can lead to self-oscillating modes. In [13], they investigated the effect of a ball valve's opening degree on flow structure and hydraulic losses, and proposed approaches to its design optimization. Furthermore, vehicle hydraulic systems often operate under various operating conditions - changing load, speed, and temperature. CFD models allow analysis of these conditions in a virtual environment and system optimization by changing geometry and operating parameters [14].

Thus, in developing vehicle hydraulic systems, CFD modeling is an important technology that speeds up design, reduces testing, enables early detection of flow problems, and improves system efficiency. Unlike other studies, this article provides a comprehensive comparison of CFD modeling results, MATLAB/Simulink simulations, and experimental data for a hydraulic ball throttle. The schematic diagram of the KI 4815M hydraulic test bench with the specified throttle control methods (Figure 1) includes: pump P with drive motor M, hydraulic cylinder C, hydraulic distributor D (four-way, three-position with manual control), hydraulic throttle DR, relief valve KP, filter F, pressure gauges MN1...MN2, and hydraulic tank T.

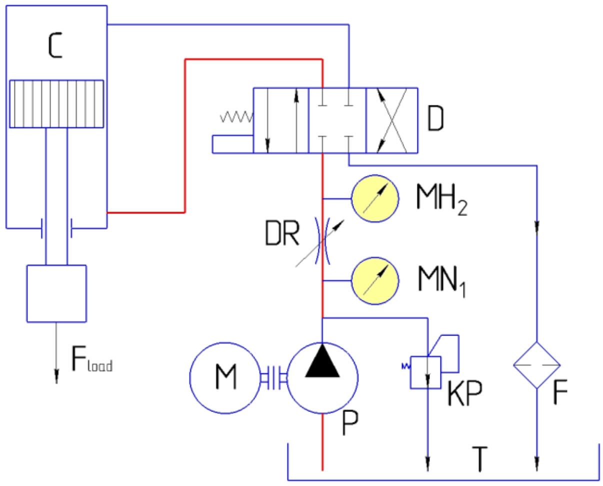

Figure 1. Schematic diagram of the KI 4815M hydraulic test bench with a DR throttle installed at the C hydraulic cylinder inlet.

The ball throttle creates a complex turbulent flow, which directly affects the stability and operation of the hydraulic drive. The presence of a sharp narrowing of the flow, turbulence, and localized pressure drops leads to:

- pressure and flow fluctuations, which can cause unstable operation of the hydraulic cylinders;
- increased load on the pump and valves, which reduces the service life of hydraulic system components;
- difficulties in accurately adjusting the speed and force of actuators. Classic analytical methods do not allow for a detailed consideration of these effects.

CFD modeling provides:

- accurate prediction of pressure drop and velocity distribution, which is important for assessing the stability of the hydraulic drive;
- visualization of turbulence zones and possible turbulent pulsations affecting actuator vibrations;
- analysis of the effect of throttle geometry on flow stability and the possibility of design optimization to reduce vibrations. According to the literature, CFD-based prediction of local resistances achieves 85–95% accuracy and provides a reliable assessment of the throttle's impact on hydraulic system stability [15, 16].

2. Formulation of the Problem

The system describing the dynamics of a hydraulic drive consists of differential equations for the motion of the moving parts, an equation for the flow of the working fluid in the hydraulic drive elements, and a flow equation. The equations of motion for the moving elements of a hydraulic cylinder are based on the equilibrium of the moving element under applied forces and moments. We assume that the working fluid‘s properties (temperature, density, viscosity, and undissolved air content) remain constant during the transient process, and that there are no leaks or cavitation. We ignore compressibility in the return pipe.

The fluid flow rate through the throttle is determined according to [17]:

$$Q = c_0 A\sqrt{\frac{2\Delta p}{\rho}}, \tag{1}$$

where c_0 is the flow rate coefficient, Δp - is the pressure drop, ρ is the working fluid density, A is the flow channel area for a ball throttle, and $A(\theta) = A_{max}\sin(\theta)$ for a spool throttle; $A = by_s$ A_{max} is the section in the fully open state, θ is the valve opening angle. y_s is the spool displacement, b is the spool valve window.

The pressures in the cavities of the hydraulic cylinder are determined by the following expressions:

$$\begin{aligned} \dot{p}_a &= \frac{E'}{V_A(y_{p0}+y_p)A_p}\left[Q_a - A_p\dot{y}_p\right], \\ \dot{p}_b &= \frac{E'}{V_B(y_{p0}+y_p)A_s}\left[Q_b - A_s\dot{y}_p\right], \end{aligned} \tag{2}$$

where V_A, V_B are the volumes of the pipelines on the rodless A and rod B cavities of the hydraulic cylinder, respectively; E' is the reduced modulus of elasticity of the working fluid, which can be determined according to [18]

$$E' = 0{,}5E_{max}lg\left(c_1\frac{p}{p_{max}} + c_2\right). \tag{3}$$

We write the flow rates Q_a and Q_b of the spool valve in the following form [19]:

$$\begin{aligned} Q_a &= c_0\left[sg(y_s)sign(p_p - p_2)\sqrt{|p_p - p_2|} - sg(-y_s)sign(p_2 - p_c)\sqrt{|p_2 - p_c|}\right] \\ Q_b &= c_0\left[sg(y_s)sign(p_3 - p_c)\sqrt{|p_3 - p_c|} - sg(-y_s)sign(p_p - p_3)\sqrt{|p_p - p_3|}\right], \end{aligned} \tag{4}$$

$$sign(y_s) = \begin{cases} 1, & for\ y_s > 0, \\ 0, & for\ y_s = 0, \\ -1, & for\ y_s < 0, \end{cases}$$

The equation of motion of the spool valve is:

$$\ddot{y}_s + 2\zeta\omega_n\dot{y}_s + \omega_n^2 y_s = \omega_n^2 u, \tag{5}$$

where u is the control action from the electromagnet; ω_n- is the natural frequency.

The equations of motion of moving elements of the hydraulic cylinder are based on the equilibrium of the moving element under applied forces and moments. For a hydraulic cylinder, it is written according to [20, 21, 22] in the following form:

$$m_p\frac{d^2y_p}{dt^2} = p_aA_p - p_bA_s - \left(F_{fr}sign\frac{dy_p}{dt} + k_v\frac{dy_p}{dt}\right) - F_{load}, \tag{6}$$

where m_p is the mass of the moving parts reduced to the piston; y_p is the piston displacement, F_{load} is the external load force, A_p, A_s are the active areas on the rodless and rod ends of the hydraulic cylinder, F_{fr} is the modulus of the dry friction force; k_v is the coefficient of viscous friction of the piston against the cylinder walls.

3. Construction of a Simulation Model

Based on the above relations (1)-(6), a simulation model of the hydraulic system with the following parameter values was developed in the Matlab-Simulink package (Table 1). The

Simulink model of the hydraulic system consists of the following subsystems: “Ball throttle,” “Hydraulic distributor,” and “Hydraulic cylinder” (Figure 2). In the “Hydraulic distributor” subsystem, the flow rates Q_a and Q_b are determined based on the input pressure and the tank pressure using Eq. (4).

Table 1. The basic simulation parameters

Parameter	Value
Hydraulic cylinder piston diameter, *mm*	75
Hydraulic cylinder rod diameter, *mm*	30
Maximum hydraulic cylinder rod stroke, *mm*	200
Weight of piston rod, *kg*	3,5
Spool valve inlet pressure, *MPa*	16
External load, *N*	700
Distributor spring natural frequency, s^{-1}	(300÷500)
Damping coefficient	(0,7÷1)
Reduced modulus of elasticity of the working fluid, *MPa*	1.8
Fluid flow rate coefficient	0.7
Viscous friction coefficient, *N*	376
Dry friction coefficient, *N*	247

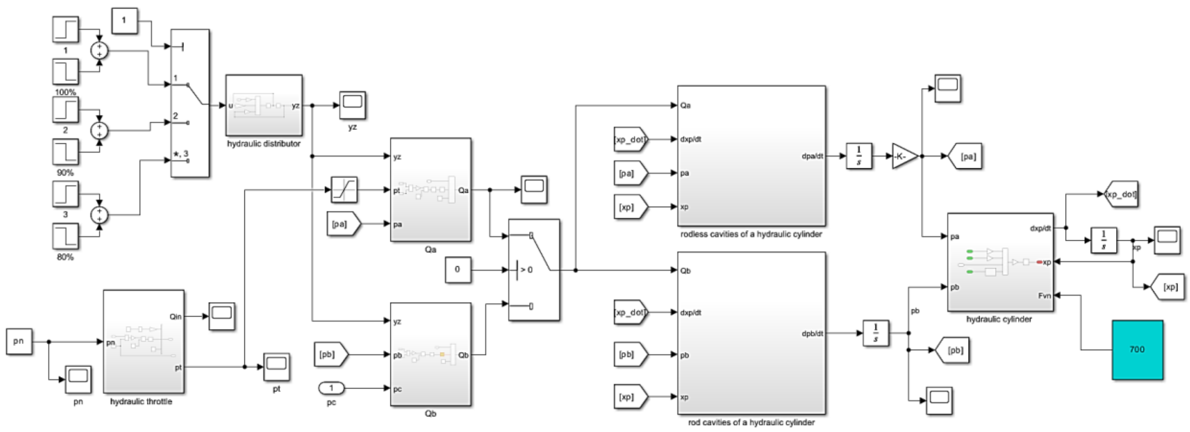

Figure 2. General view of the Simulink model of the hydraulic system

4. CAD MODEL CONSTRUCTION METHOD

The 3D model of the throttle and piping sections of the hydraulic system was created in SolidWorks [23] based on the actual dimensions of the experimental setup (Figure 3).

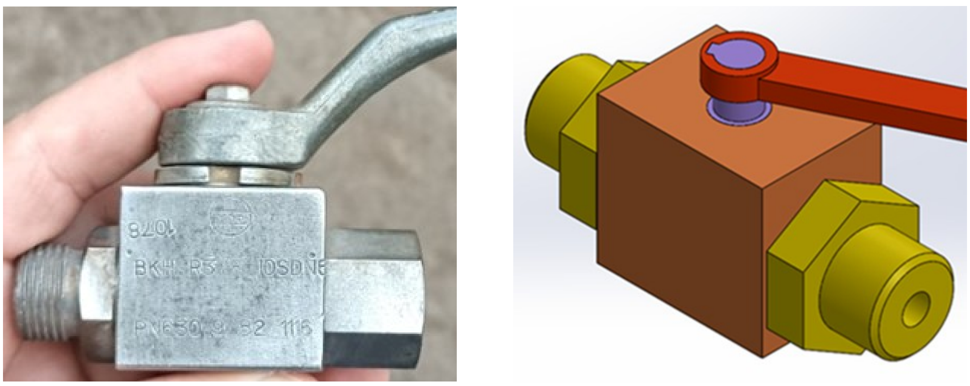

a) b)

Figure 3. Ball throttle: a) test bench throttle; b) 3D model of the throttle

CFD model setup. The 3D flow domain was discretized in SolidWorks Flow Simulation using an adaptive Cartesian mesh with local refinement near the ball throttle orifice and solid walls to resolve the high velocity gradients in that region. Turbulence was modeled using the standard k-ε model with standard wall functions. The following boundary conditions were applied: a specified inlet pressure/velocity corresponding to the pump flow rate at the inlet, atmospheric static pressure at the outlet, and no-slip conditions on all solid walls. The working fluid was treated as incompressible with constant density and viscosity, consistent with the assumptions adopted in the simulation model. The solution was considered converged when the residuals for mass, momentum, and turbulence quantities dropped below $10^{-3}÷10^{-4}$, together with stabilization of the monitored outlet pressure and mass flow rate.

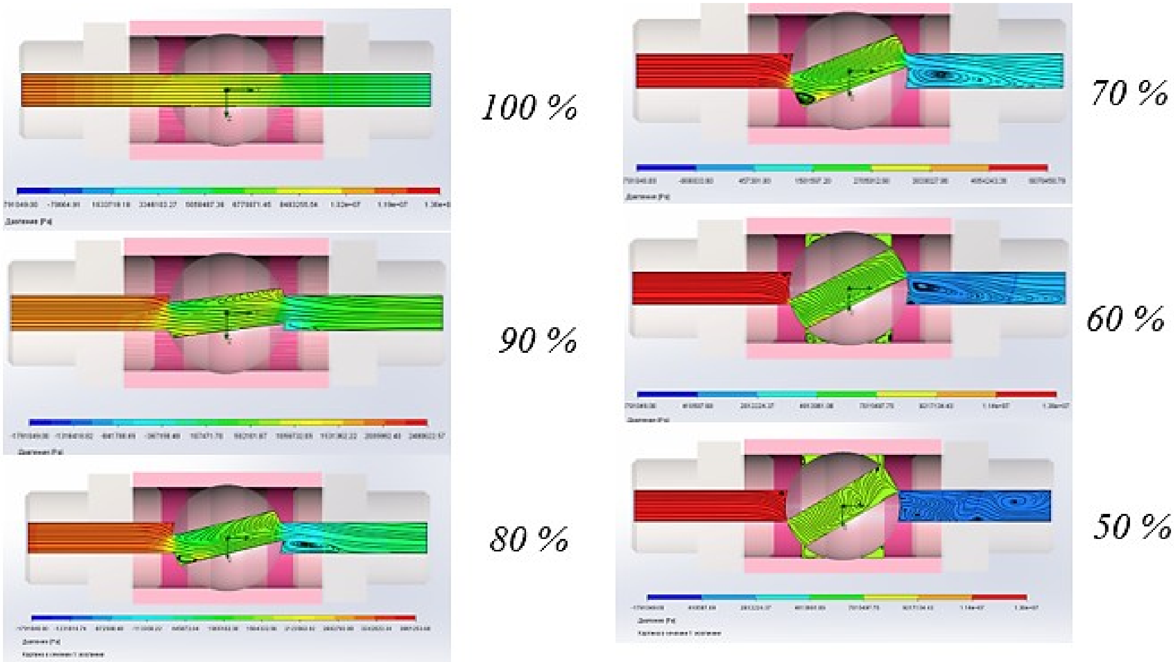

Figure 4. Channel pressure isolines for various ball throttle openings

Figure 4 shows the channel pressure isolines for various ball throttle openings. The CFD results for flow through the ball throttle, considering its geometry, are compared with experimental data measured on the KI 4815M hydraulic test bench to verify the accuracy of the calculations and analyze the throttle's impact on hydraulic system stability.

5. Experimental Study

The study focused on the KI 4815M test rig's hydraulic circuit. A pump supplies the working fluid, which passes through a ball throttle and enters a hydraulic cylinder. SS302 diaphragm sensors connected to an Arduino analog-to-digital converter (ADC) measured pressure. The SS302 piezoresistive pressure sensor has an accuracy of ±0.5% F.S. (including non-linearity, hysteresis, and repeatability), a response time of less than 4 ms, and a temperature coefficient of ±0.03% F.S./°C; the pressure range used for the present test bench corresponds to the working pressure of the KI-4815M hydraulic circuit. The Arduino-based data acquisition system employs a 10-bit ADC (0÷1023 counts), providing a voltage resolution of approximately 4.88 mV at a 5 V reference.

The preparation of the computer-controlled measuring systems of the KI-4815M hydraulic test bench consists of the following stages: selection and placement of sensors (mechanical-toelectrical converters or vice versa); preliminary processing of analog signals; conversion of analog signals to digital; classification and storage of measured values or their preliminary processing; software for mathematical processing and analysis of the obtained results. Figure 5 shows the functional diagram of the measuring system connections to the computer.

During distributor operation on the KI-4815M test bench a hydraulic pump of appropriate capacity is installed. A control check of the distributor consists of determining the actuation pressure of the relief valve and the spool return mechanism. The tightness of the housing components and oil leakage in the valves are checked.

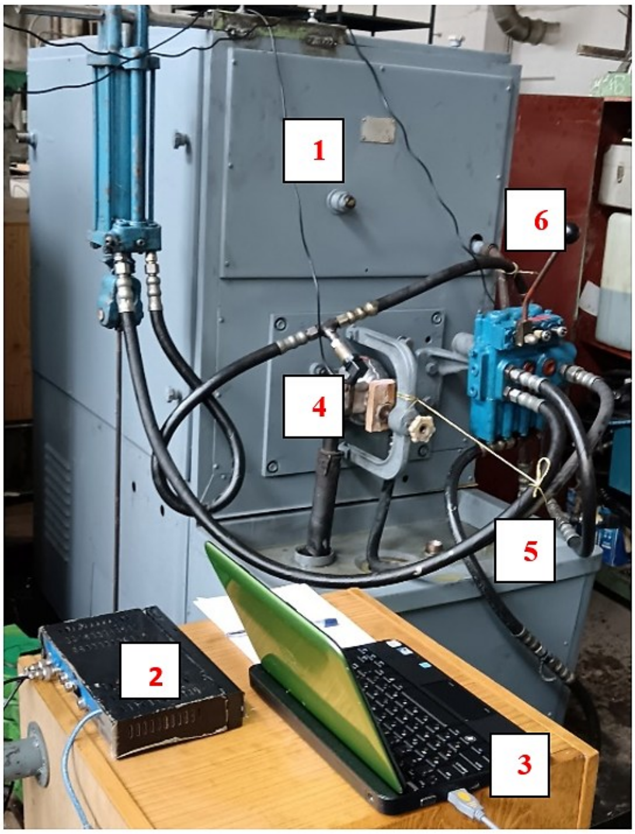

Figure 5. Functional diagram of the connections of the measuring system to the computer of the KI 4815M bench. 1 – KI-4815M bench; 2 – Arduino analog-to-digital converter (ADC); 3 – laptop computer; 4, 5 – pressure sensors; 6 – ball throttle

To quantify the measurement uncertainty, each pressure reading was repeated three times (n = 3) at every throttle opening. For each measurement point, the sample mean and sample standard deviation were calculated, and the 95% confidence interval was obtained using the Student's t-distribution $\left(t_{0,9752} = 4{,}303\right)$ as $\Delta = \frac{ts}{\sqrt{n}}$. The resulting uncertainty does not exceed ±0.16 MPa at the throttle inlet and ±0.02 MPa at the throttle outlet (relative uncertainty below 7,1% at all measurement points, and below 2% for the majority of them), confirming a high level of measurement repeatability. Figures 6 and 7 show the corresponding confidence intervals as error bars on the experimental points.

6. RESULTS ANALYSIS

Figure 4 shows pressure isolines in the channel for different ball-throttle openings. A noticeable narrowing of the jet, followed by an expansion, occurs in the area of the throttle's flow opening. Maximum velocity gradients occur at the minimum-flow section, accompanied by a significant pressure drop. This pressure drop is the primary source of hydraulic losses in the throttle. The pressure fields illustrate a distinct difference between the inlet and outlet cavities. A zone of high pressure is formed at the inlet, while a sharp decrease in pressure is observed downstream of the throttle. At small openings (50÷60%), the pressure drop is greatest because of increased local resistance and higher flow turbulence. Moreover, the velocity-field analysis reveals local vortex structures behind the edge of the spherical opening. These vortices contribute to additional energy losses and can generate pressure pulsations within the hydraulic system. As the throttle opening increases, vortex formation weakens, and the flow structure becomes more orderly.

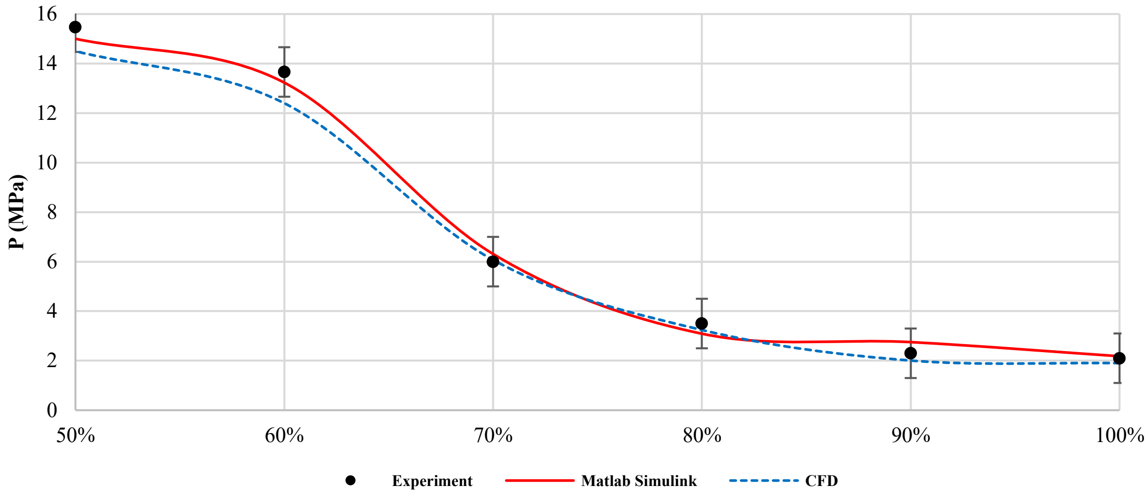

Figure 6. Temporary changes in pressure at the throttle inlet at a load of Fload=700 N

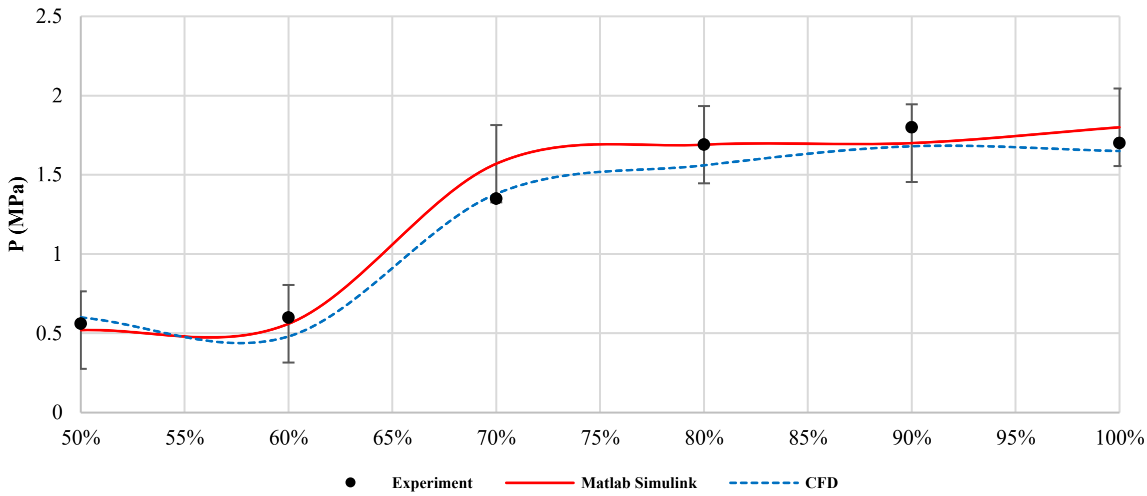

Figure 7. Temporary changes in pressure at the throttle outlet at a load of Fload=700 N

Figures 6 and 7 show the pressure dependence at the ball throttle inlet and outlet, respectively, under a load of Fload=700 N. Comparing the graphs allows us to evaluate the impact of throttling on the system's hydrodynamic processes. Analysis revealed that the pressure at the throttle inlet (Figure 6) is higher and characterized by noticeable pulsations, especially at small openings (50÷60%). This is due to the throttle's increased hydraulic resistance, which causes pressure buildup upstream of the flow area. Meanwhile, the pressure at the throttle outlet (Figure 7) is significantly lower and smoother. The observed pressure drop confirms a pressure drop across the throttle, which regulates the working-fluid flow. As the throttle opening increases from 70% to 100%, the pressure drop decreases, accompanied by a reduction in pulsation amplitude at both the inlet and outlet of approximately 31÷35% (rising to approximately 13÷15% when the full 50÷100% opening range is considered). This indicates reduced local hydraulic losses and more stable flow.

A comparison of the results from MATLAB/Simulink, CFD, and experiment showed good agreement at the vibronic measurement points. The discrepancy does not exceed 5,67% at a load of $F_{load}=700\ N$, confirming the adequacy of the developed model and the reliability of the CFD calculations. The ball throttle creates a controlled pressure differential between the inlet and outlet, facilitating flow regulation and reducing dynamic oscillations in the hydraulic drive as the throttle opening increases.

7. Conclusion

The ball throttle establishes a stable pressure differential and effectively regulates the working-fluid flow rate. As the throttle opening increases, the amplitude of pressure pulsations decreases, stabilizing the flow. Specifically, based on the inlet pressure data, the pulsation amplitude decreases by approximately 13÷15% as the throttle opening increases from 50% to 100%, and by approximately 31÷35% between 70% and 100% opening, consistently across the experimental, MATLAB/Simulink, and CFD results, confirming a substantial improvement in hydraulic drive stability. A comparison of CFD modeling, simulation, and experimental results showed a strong correlation, with the maximum discrepancy not exceeding 5,67% at a load of 700 *N*. This confirms the accuracy of the developed models and the reliability of the obtained results.

Acknowledgments

We express our sincere gratitude to the Academy of Sciences of the Republic of Uzbekistan for their ongoing support.

References

[1] Avrunin GA, Gritsai IV, Kirichenko IG, Moroz II, Shcherbak OV (2008) Volumetric hydraulic drive and hydropneumatic automation. KhNADU, Kharkov.

[2] Anderson JD (2017) Computational Fluid Dynamics: The Basics with Applications. McGraw-Hill.

[3] Versteeg H, Malalasekera W (2007) An Introduction to Computational Fluid Dynamics. Pearson.

[4] Domagala M, Fabis-Domagala J (2023) A review of the CFD method in the modeling of flow forces. Energies, 16:6059.

[5] Musa AA, et al. (2021) Advances in CFD-driven design for fluid-particle separation and filtration systems in engineering applications. Iconic Research and Engineering Journals, 5(3):347-365.

[6] Ahmed R, Motin A, Srinivasan C, Zhang Y (2022) CFD analysis of a centrifugal pump controlling a vehicle coolant hydraulic system: A comparison between MRF and transient approaches. SAE Technical Paper.

[7] Tamburrano P, et al. (2019) 2D CFD analysis of servovalve main stage internal leakage. Proceedings of the ASME/BATH 2019 Symposium on Fluid Power and Motion Control, Longboat Key, FL, USA.

https://doi.org/10.31436/iiumej.v27i3.4503

[8] Frosina E, Senatore A, Buono D (2015) 3D CFD transient analysis of the forces acting on the spool of a directional valve. Energy Procedia, 81:1090-1101.

[9] Herakovič N, Duhovnik J, Šimic M (2015) CFD simulation of flow force reduction in hydraulic valves. Tehnički Vjesnik, 22(2):453-463.

[10] Wu D, Li S, Wu P (2015) CFD simulation of flow-pressure characteristics of a pressure control valve for automotive fuel supply system. Energy Conversion and Management, 101:658-665.

[11] Yu J, Zhuang J, Yu D (2014) Modeling and analysis of a rotary direct drive servovalve. Chinese Journal of Mechanical Engineering, 27(5):1064-1074.

[12] Bazsó C, Hős C (2012) A CFD study on the stability of a hydraulic pressure relief valve. Conference on Modeling Fluid Flow (CMFF'12), Budapest, Hungary.

[13] Wang JX, Li FX (2020) Flow analysis and structural optimization of a ball valve focusing on the effects of opening degree. Academic Journal of Manufacturing Engineering, 18(2):76-86.

[14] White FM (2016) Fluid Mechanics. McGraw-Hill.

[15] Çengel Y, Cimbala J (2020) Fluid Mechanics: Fundamentals and Applications. McGraw-Hill.

[16] Menter F (1994) Two-equation turbulence models for engineering applications. AIAA Journal, 32(8):1598-1605.

[17] Avtushko VP, et al. (2015) Theory and design of hydraulic-pneumatic drives. Part 1. Two-position hydraulic-pneumatic drives with relay control. BNTU, Minsk.

[18] Šulc B, Jan JA (2002) Non linear modelling and control of hydraulic actuators. Acta Polytech., 42(3):41-47.

[19] Jelali M, Kroll A (2012) Hydraulic Servo-Systems: Modelling, Identification and Control. Springer Science & Business Media.

[20] Petrov VV (1951) On self-oscillations of two-cascade servo mechanisms with relay control. Automation and Telemechanics, 12:1-28.

[21] Khokhlov VA, et al. (1971) Electrohydraulic servo systems. Mashinostroenie, Moscow.

[22] Metlyuk NF, Avtushko VP (1980) Dynamics of pneumatic and hydraulic drives of automobiles. Mashinostroenie, Moscow.

[23] SolidWorks Corporation (2022) Flow Simulation Technical Reference. Dassault Systèmes.